

Closed-Form Expressions for Two- and Three-Colorable States

Konstantinos-Rafail Revis, Hrachya Zakaryan, and Zahra Raissi*

Department of Computer Science, Paderborn University,

Warburger Str. 100, 33098, Paderborn, Germany

Institute for Photonic Quantum Systems (PhoQS), Paderborn University,

Warburger Str. 100, 33098 Paderborn, Germany

Graph states are a class of multi-partite entangled quantum states, where colorability, a property rooted in their mathematical foundation, has significant implications for quantum information processing. In this study, we investigate the colorability of graph states in qudit systems to simplify their representation and enhance their practical applications. We present closed-form expressions for all two-colorable graph states. Our findings show that the closed-form expression of these states is tightly linked to the graph structure and the distribution of particles in red (n_R) and blue (n_B). Additionally, we explore a broad family of three-colorable graph states constructed from two two-colorable graph states. The closed-form expression for these states is in the form of one two-colorable state tensor product with the graph basis formed from another two-colorable state. Our approach systematically reduces the number of terms required to represent these states. Furthermore, we demonstrate that many well-known mathematical graphs, including friendship graphs, fit within our formalism. Finally, we discuss the LU/SLOCC (Local Unitary/Stochastic Local Operation and Classical Communication) equivalence between two- and three-colorable graph states. Our findings have broad implications for characterizing the LU/SLOCC equivalence of graph state classes and pave the way for future research.

I. INTRODUCTION

Multipartite entanglement lies at the core of quantum information theory. In recent years, substantial efforts have been made to characterize the entanglement properties of multipartite quantum states and to construct new examples of highly entangled states [1–12]. In this work, we focus on a specific class of multipartite entangled states called graph states [13], which are pure quantum states defined based on a graph. The bijection between graph states and stabilizer states, as proved in [14], highlights the wide range of applications for which graph states are ideal candidates. These applications include measurement-based quantum computing [15, 16], quantum networks [17], and quantum error-correcting codes [18, 19].

Given the construction of graph states, it is reasonable to examine whether certain properties well-studied in classical graph theory reflect physical properties of graph states. One such property is the chromatic number, which is the minimal number of colors needed to color the vertices such that no two adjacent vertices share the same color [20]. In this work, the term "colorability" refers to the chromatic number of the graph. Historically, most studies have focused on two-colorable graphs. A crucial question is whether the colorability of graph states encodes deeper physical meanings. This question has largely been unexplored in previous works. One notable exception is [21], which shows that almost all two-colorable graph states have maximal Schmidt measures.

In this work, we aim to present closed-form expressions for all two-colorable graph states. Our approach

demonstrates a systematic method to transform these states into forms with fewer terms in the computational basis, tightly linked to the graph structure representing them. Our analysis is then extended to a broad family of three-colorable graph states, illustrating that the colorability of graph states is connected to the endeavor of finding the minimum number of terms in the computational basis to represent the state. We provide a broad family of interesting examples, many of which are graphs extensively studied in classical graph theory. Finally, we study the obtained results under the scope of possible equivalency under local transformations [22–27] between the two- and three-colorable graph states. Our framework encompasses various existing works, including efforts to develop concrete methodologies for providing low-particle counterexamples to the LC-LU conjecture [28, 29]. The LC-LU conjecture pertains to the equivalence of graph states under local Clifford (LC) operations and local unitary (LU) operations. Consequently, part of this work is dedicated to presenting some of these examples and proposing a set of implementable approaches.

II. BASICS OF QUDIT GRAPH STATES

Let us start our discussion with the mathematical notion of graphs [30, 31], a group of vertices connected by an edge. A graph can be represented using a diagram in the plain. In this context, we are interested in the physical systems will be the vertices while the edges will denote their interaction. Therefore it is typical to call the vertices, also as particles, or different labs. A formal definition of an undirected and finite graph is a pair of $G = (V, E)$ of the finite set $V \subset \mathbb{N}$ and a set $E \subset [V]^2$. The elements of V are called vertices, while edges are

* zahra.raissi@uni-paderborn.de

the elements of E . Two vertices $i, j \in V$, with a total number of vertices being N , are called adjacent if they are the endpoint of an edge. This allows us to define the adjacency matrix Γ , which is a symmetric $N \times N$ matrix. It has to be noted that we are working only with connected diagrams. In this work, we focus on graph states. Particularly, when qudits are assumed, the adjacency matrix Γ has elements Γ_{ij} for $i, j \in V$. These elements, denoted $\theta_{ij} \in \mathbb{F}_d$, with \mathbb{F}_d a finite finite field of dimension d . Bearing these in mind the adjacency matrix is defined as[32]:

$$\Gamma_{ij} = \begin{cases} \theta_{ij} & \text{if } i, j \in E \\ 0 & \text{otherwise} \end{cases} \quad (1)$$

Finally, mentioning the neighborhood $N_i \subset V$ is useful, which is the set of vertices for which $\{i, j\} \in V$. For a graph $G = (V, E)$ where V and E are the sets of vertices ($|V| = n$) and edges we define a graph state as:

$$|\psi_{\text{GS}}\rangle = \left(\prod_{\{k,j\} \in E} CZ_{kj} \right) |+\rangle^{\otimes n}, \quad \text{where } |+\rangle = H|0\rangle. \quad (2)$$

At this point, some example states will be presented, which are broadly used in the literature. In figure (1) a cluster state is presented, in figure (11) a complete bipartite state is given, and finally in figure (18) the star-shape graph is depicted. Let us briefly discuss the

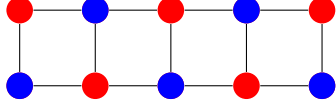


FIG. 1. Cluster state with 2-colorable vertices. Red and blue colors indicate the two different vertex sets. There are $n_R = 5$ red particles and $n_B = 5$ blue particles.

qudits[11, 33], which were mentioned before and they are systems with d levels. The Hilbert space of every particle is \mathbb{C}^d . Let assume that $a \in \mathbb{F}_d$. The Pauli operators X and Z acting on the eigenstates of Z are acting as follows:

$$X^a|i\rangle = |i+a\rangle \quad \text{and} \quad Z^a|i\rangle = \omega^{ia}|i\rangle, \quad (3)$$

with $\omega = e^{i2\pi/d}$ and every addition is performed with modular arithmetic d . Therefore, $X^d = \mathbb{I}_d$ and $Z^d = \mathbb{I}_d$, with \mathbb{I}_d the identity matrix of dimension d . Let us continue discussing two joined operators extensively used in this work, the control-Z operator:

$$C_1 Z_2^a |i\rangle_1 |j\rangle_2 = \omega^{ija} |i\rangle_1 |j\rangle_2. \quad (4)$$

In this case, the indices in the CZ indicate that the control operation is taking place in the first particle and the Z-operator is applied on the second particle when it is necessary. In any case, CZ is a symmetric operation and in principle, these indices can be omitted. They are used for clarity purposes in our proofs. Similar is the indices

notation for the control-X operator, while in this case the indices are necessary and can not be omitted:

$$C_1 X_2^a |i\rangle_1 |j\rangle_2 = |i\rangle_1 |i+j+a\rangle_2. \quad (5)$$

Another operator that will be extensively used is the Hadamard operator:

$$H|i\rangle = \sum_{l=0}^{d-1} \omega^{il} |l\rangle, \quad \text{and} \quad H^\dagger |i\rangle = \sum_{l=0}^{d-1} \omega^{-il} |l\rangle. \quad (6)$$

Finally, some useful relations for the upcoming results are presented in A.

III. 2-COLORABLE GRAPH STATES CLOSED-FORM EXPRESSION

Let $|\psi_{\text{2-color}}\rangle$ be a two-colorable graph. Therefore two sets of vertices can be assumed. With B the set of blue vertices are denoted and with R the set of red vertices are denoted. It has to be underlined that depending on the goal or the application a graph state is used the vertices are also called particles or labs. Let us also define the total number of the red vertices to be n_R and the total number of blue vertices to be n_B . The total number of vertices in the graph is $n = n_R + n_B$.

If it is considered that the control operation is always taking place in the red vertices and the target particles are always the blue. Therefore $|\psi_{\text{GS}}\rangle$, it is given as follows:

$$|\psi_{\text{GS}}\rangle = \prod_{r \in R, b \in B} C_r Z_b^{\Gamma_{rb}} |+\rangle^{\otimes R} |+\rangle^{\otimes B} \quad (7)$$

At this point, H^\dagger is performed on blue vertices. It is also assumed without loss of generality that $n_B > n_R$. Therefore the following is obtained (the normalization factor is omitted for simplicity):

$$\begin{aligned} H^{\dagger \otimes B} |\psi_{\text{2-color}}\rangle &= \prod_{r \in R, b \in B} H^{\dagger \otimes B} C_r Z_b^{\Gamma_{rb}} |+\rangle^{\otimes R} |+\rangle^{\otimes B} \\ &= \prod_{r \in R, b \in B} C_r X_b^{\Gamma_{rb}} |+\rangle^{\otimes R} H^{\dagger \otimes B} H^{\otimes B} |0\rangle^{\otimes B} \\ &= \prod_{r \in R, b \in B} C_r X_b^{\Gamma_{rb}} |+\rangle^{\otimes R} |0\rangle^{\otimes B} \\ &= \sum_{i_1, \dots, i_{n_R}=0}^{d-1} \prod_{r \in R, b \in B} C_r X_b^{\Gamma_{rb}} |i_1 \dots i_{n_R}\rangle |0\rangle^{\otimes B} \\ &= \sum_{i_1, \dots, i_{n_R}=0}^{d-1} \prod_{r \in R, b \in B} |i_1 \dots i_{n_R}\rangle X_b^{\Gamma_{rb} * i_r} |0\rangle^{\otimes B} \\ &= \sum_{i_1, \dots, i_{n_R}=0}^{d-1} \prod_{b \in B} |i_1 \dots i_{n_R}\rangle X_b^{\sum_{r \in R} \Gamma_{rb} * i_r} |0\rangle^{\otimes B} \\ &= \sum_{i_1, \dots, i_{n_R}=0}^{d-1} |i_1 \dots i_{n_R}\rangle \bigotimes_{b \in B} |\sum_{r \in R} \Gamma_{rb} * i_r\rangle \end{aligned}$$

At this point, the following for the adjacency matrix of a two-colorable graph state must be recalled:

$$\Gamma_{\text{2-color}} = \left(\begin{array}{c|c} \text{B} & \text{R} \\ \hline O & A_{RB} \\ \hline A_{RB}^T & O \end{array} \right) \quad (8)$$

It is clear that the block with zero has every combination of vertices with the same color, which by definition is zero. The block A_{RB} represents the $n_R \times n_B$ matrix that contains the weights of every combination between the red and the blue vertices. Let us define $\vec{i} = (i_1, i_2, \dots, i_{n_R})$ and $\mathcal{G} = [\mathbb{I}_{n_R} \mid A_{RB}^T]$, where \mathbb{I}_{n_R} is the identity matrix of order n_R . A careful inspection of the outcome of $H^{\dagger \otimes B} |\psi_{\text{2-color}}\rangle$ let us write:

$$H^{\dagger \otimes B} |\psi_{\text{2-color}}\rangle = \sum_{i_1, \dots, i_{n_R}=0}^{d-1} |\vec{i} \mathcal{G}^T\rangle \quad (9)$$

The above equation is a helpful compact form of every two-colorable graph and has gripping consequences which are going to be discussed in the upcoming section.

A. Discussion of the closed-form expression for the 2-colorable graph.

In this subsection let us discuss the impact of the obtained result. The first is that the number of terms needed to describe the 2 colorable states $|\psi_{\text{2-color}}\rangle$ can be reduced from d^n to d^{n_R} for every 2-colorable graph state. This result is important because it provides a lower bound in comparison with the one found in the [32] where the general lower bound for the minimal number of terms needed for the general setup was $\lfloor \frac{n}{2} \rfloor$. It is crucial to mention that the obtained result is a generalization of the results presented also in [32] regarding the minimal support. Additionally, the matrix \mathcal{G} is called generator matrix[34] and in the presented case is written in the standard form. One should note that a classical linear error-correcting code is denoted as $[n, k, d_H]_q$ if q^k messages are encoded into in space of dimension q^n , where $q^n > q^k$. Every message has a d_H Hamming distance. Linear codes are a particular category of codes described by their injective mapping from the set of messages to the set of codewords, which is both linear and founded over a finite field \mathbb{F}_d . For more details on the aforementioned topic and the connection of the graph states as well as to noteworthy families of quantum states one can refer to [35]. Furthermore, we have to recall a result we refer to in the introduction of this work but now we can discuss it in greater detail. According to [21] almost all two colorable graph states have maximal Schmidt measure. The reason for this is that the probability of an $n \times n$ matrix to be singular is given by the expression $n^2 \times 2^{-n}$ and therefore as the n increases this probability goes closer to zero. Schmidt number is defined as:

$$E_s(|\psi\rangle) = \log_2(r), \quad (10)$$

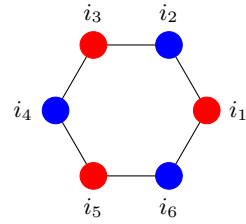


FIG. 2. The first example of the implementation of our closed form. Here we have a six-particle circle. By definition 6 independent parameters are needed to characterize the state.

where r is the number of terms in an expansion of the state in product basis. Therefore a crucial question left for future research is whether this is also the minimal support of $|\psi_{\text{2-color}}\rangle$, which means if this is the minimal number of terms every two-colorable graph can be written. Last but not least the connection of our result with the orthogonal arrays must be discussed [36]. An orthogonal array, denoted as OA(r, N, d, k), is an arrangement composed by r rows, N columns, and entries taken from the set $\{0, \dots, d-1\}$. Every subset of k columns contains all possible combinations of symbols, occurring the same number (λ) of times along the rows. Two OA are called equivalent if one array can be transformed into the other one by applying permutations or relabelling of symbols in rows or columns. It is crystal clear that every 2-colorable graph state can be written as an OA. The above arguments strengthen the value of the obtained result.

B. Examples of the usage of the obtained closed-form

At this point let us present some useful examples of how our formula can be used. Assuming a graph state with the corresponding graph given in the figure (2), where the state is given by the following equation:

$$|\Psi_{GS}\rangle = \sum_{i_1, \dots, i_6=0}^{d-1} \omega^{i_1 i_2} \omega^{i_2 i_3} \omega^{i_3 i_4} \omega^{i_4 i_5} \omega^{i_5 i_6} \omega^{i_6 i_1} |i_1, i_2, i_3, i_4, i_5, i_6\rangle$$

After the implementation of our formalism, the state obtained is given by the following equation:

$$|\psi_{\text{closed-form}}\rangle = \sum_{i,j,k=0}^{d-1} |i, i+j, j, j+k, k, i+k\rangle \quad (11)$$

To understand how the indices work we have to pick the color with fewer indices, in this case, the blue and the red particles have the same number of particles but the general construction approach remains the same. Therefore we use the free indices i, j and k on the red particles. For the indices of the blue particles, we have to add the free indices of the neighbors as depicted in the figure.

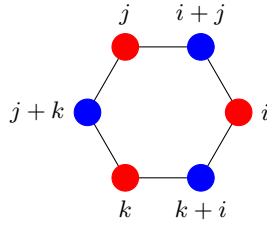


FIG. 3. Implementation of the closed form we developed on the six-particle circle. To obtain the closed form one has to assign the free indices to the color that has fewer particles. Note that in this case, red and blue particles exist in the same amount but still the methodology provided is valid. After assigning the free indices to the red, in this case, without loss of generality, the indices of the blue particles emerge by adding the indices of the corresponding neighboring vertices.

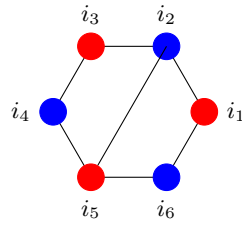


FIG. 4. A six-particle ladder cluster state before the implementation of the obtained closed-form and the corresponding methodology of assigning indices based on the color of the particle. By definition 6 independent parameters are needed to characterize the state.

By construction, the neighbors must be red particles. The construction approach is general for any two-colorable graph. For clarification, another useful example is assuming the graph given in figure 4, which is a ladder cluster state that has 6 particles, and the corresponding state using the definition of graph states is:

$$|\Psi_{GS}\rangle = \sum_{i_1, \dots, i_6=0}^{d-1} \omega^{i_1 i_2} \omega^{i_2 i_3} \omega^{i_3 i_4} \omega^{i_4 i_5} \omega^{i_5 i_6} \omega^{i_6 i_1} \omega^{i_2 i_5} |i_1, i_2, i_3, i_4, i_5, i_6\rangle$$

After our closed form is implemented we have the closed-form obtained by the following equation:

$$|\psi_{\text{closed-form}}\rangle = \sum_{i,j,k=0}^{d-1} |i, i+j+k, j, j+k, k, i+k\rangle \quad (12)$$

The construction of the indices to obtain the above equation is the one explained before and the corresponding figure is:

IV. 3 COLORABLE CZ GRAPH STATES

We proceed with our analysis of the three colorable graph states. Before we start it is crucial to note that

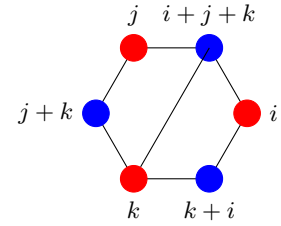


FIG. 5. The first example of the implementation of our closed form. Here we have a six-particle ladder cluster state. By definition 6 independent parameters are needed to characterize the state.

the 3-coloring is an NP-hard problem [37–39]. In the presented case not every three-colorable graph is assumed. To create the three-colorable graph state $|\psi_{\text{3-color}}\rangle$ we are interested it is assuming that the set of the blue vertices, the assumption that $n_B > n_R$ still holds without a loss of generality for the following proof, is separated into sets B_c , which are n_{B_c} in total and B_u , which are n_B in total. The set B_c denoted the blue particles which remain connected to the red particles but they are also connected to each other and they create a new 2-colorable graph. The vertices belonging to B_u remain unaffected as they were in the 2-colorable graph state $|\psi_{\text{2-color}}\rangle$. It is also clear that the total number of particles is $n = n_B + n_R = n_{B_c} + n_{B_u} + n_R$. Bearing in mind this information $|\psi_{\text{3-color}}\rangle$ is defined as following:

$$|\psi_{\text{3-color}}\rangle = \left(\prod_{b, b' \in B_c} C_b Z_{b'}^{\Gamma_{bb'}} \right) \left(\prod_{b \in B_c, r \in R} C_b Z_r^{\Gamma_{br}} \right) \left(\prod_{b \in B_u, r \in R} C_b Z_r^{\Gamma_{br}} \right) |+\rangle^{\otimes R} |+\rangle^{\otimes B_u} |+\rangle^{\otimes B_c}. \quad (13)$$

It must be underlined that the normalization factor will be omitted during the proof. Following the steps of the proof for the closed form of the $|\psi_{\text{2-color}}\rangle$, $H^{\dagger \otimes B} = H^{\dagger \otimes B_c} H^{\dagger \otimes B_u}$ is applied:

$$H^{\dagger \otimes B_c} H^{\dagger \otimes B_u} |\psi_{\text{3-color}}\rangle = \left(H^{\dagger \otimes B_c} \left(\prod_{b, b' \in B_c} C_b Z_{b'}^{\Gamma_{bb'}} \right) \left(\prod_{b \in B_c, r \in R} C_b Z_r^{\Gamma_{br}} \right) \right) \left(H^{\dagger \otimes B_u} \left(\prod_{b \in B_u, r \in R} C_b Z_r^{\Gamma_{br}} \right) |+\rangle^{\otimes R} |+\rangle^{\otimes B_u} |+\rangle^{\otimes B_c} \right). \quad (14)$$

It is clear that:

$$H^{\dagger \otimes B_u} \left(\prod_{b \in B_u, r \in R} C_b Z_r^{\Gamma_{br}} \right) |+\rangle^{\otimes R} |+\rangle^{\otimes B_u} = \sum_{u_1, \dots, u_{n_R}=0} |u_1, \dots, u_{n_R}\rangle \bigotimes_{b \in B_u} \left| \sum_{r \in R} \Gamma_{rb} u_r \right\rangle. \quad (15)$$

Therefore it is possible to obtain the following:

$$H^{\dagger \otimes B_c} H^{\dagger \otimes B_u} |\psi_{3\text{-color}}\rangle = \sum_{u_1, \dots, u_{n_R}=0} H^{\dagger \otimes B_c} \left(\prod_{b, b' \in B_c} C_b Z_{b'}^{\Gamma_{bb'}} \right) \left(\prod_{b \in B_c, r \in R} C_b Z_r^{\Gamma_{br}} \right) |u_1, \dots, u_{n_R}\rangle \bigotimes_{b \in B_u} \left| \sum_{r \in R} \Gamma_{rb} u_r \right\rangle H^{\otimes B_c} |0\rangle^{\otimes B_c}. \quad (16)$$

Before proceeding with the proof it is important to note that we can write the adjacency matrix for the 2-colorable graph with vertices from B_u and R , which will be denoted as $\Gamma_{2\text{-color}, B_u}$ as:

$$\Gamma_{2\text{-color}, B_u} = \begin{pmatrix} 0 & A_u^T \\ A_u & 0 \end{pmatrix}.$$

Let us define $\vec{u} = (u_1, u_2, \dots, u_{n_R})$ and the corresponding generator matrix $\mathcal{G}_u = [\mathbb{I}_{n_R} \mid A_u^T]$, where \mathbb{I}_{n_R} is the identity matrix of order n_R . Therefore equation (16) can be written as:

$$H^{\dagger \otimes B_c} H^{\dagger \otimes B_u} |\psi_{3\text{-color}}\rangle = \sum_{u_1, \dots, u_{n_R}=0} H^{\dagger \otimes B_c} \left(\prod_{b, b' \in B_c} C_b Z_{b'}^{\Gamma_{bb'}} \right) \left(\prod_{b \in B_c, r \in R} C_b Z_r^{\Gamma_{br}} \right) |\vec{u} \mathcal{G}_u^T\rangle H^{\otimes B_c} |0\rangle^{\otimes B_c}. \quad (17)$$

However, this form is not helpful to proceed with our calculation. The primary goal is to commute $H^{\dagger \otimes B_c}$ through the two products with the control-Z operations. For this reason, the following is performed:

$$\begin{aligned} H^{\dagger \otimes B_c} \left(\prod_{b, b' \in B_c} C_b Z_{b'}^{\Gamma_{bb'}} \right) &= \\ H^{\dagger \otimes B_c} \left(\prod_{b, b' \in B_c} C_b Z_{b'}^{\Gamma_{bb'}} \right) H^{\otimes B_c} H^{\dagger \otimes B_c} &= \\ \mathcal{O}_{b, b' \in B_c} H^{\dagger \otimes B_c}. \end{aligned} \quad (18)$$

Let us proceed with our proof, by commuting the $H^{\dagger \otimes B_c}$

though $\left(\prod_{b \in B_c, r \in R} C_b Z_r^{\Gamma_{br}} \right)$:

$$\begin{aligned} H^{\dagger \otimes B_c} H^{\dagger \otimes B_u} |\psi_{3\text{-color}}\rangle &= \\ \sum_{u_1, \dots, u_{n_R}=0} \mathcal{O}_{b, b' \in B_c} \left(\prod_{r \in R, b \in B_c} C_r X_b^{\Gamma_{rb}} \right) &|u_1, \dots, u_{n_R}\rangle \\ \left(\bigotimes_{b \in B_u} \left| \sum_{r \in R} \Gamma_{rb} u_r \right\rangle \right) |0\rangle^{\otimes B_c}. \end{aligned} \quad (19)$$

The action of the $\prod_{r \in R, b \in B_c} C_r X_b^{\Gamma_{rb}}$ operators is already known, therefore:

$$\begin{aligned} H^{\dagger \otimes B_c} H^{\dagger \otimes B_u} |\psi_{3\text{-color}}\rangle &= \\ \sum_{u_1, \dots, u_{n_R}=0} |u_1, \dots, u_{n_R}\rangle \left(\bigotimes_{b \in B_u} \left| \sum_{r \in R} \Gamma_{rb} u_r \right\rangle \right) & \\ \left(\mathcal{O}_{b, b' \in B_c} \bigotimes_{b \in B_u} \left| \sum_{r \in R} \Gamma_{rb} u_r \right\rangle \right) \end{aligned} \quad (20)$$

A. Determination of the action of $\mathcal{O}_{b, b' \in B_c}$ operator

Let us start our analysis by defining that $\sum_{r \in R} \Gamma_{rb} u_r = f_k$. It is also important to recall that by construction the B_c is assumed to be a 2 colorable graph, and thus the total graph is a three-colorable one. This means that the B_c graph has particles that maintain their blue color. These particles belong to a set which we are going to denote as B' and this is a set with elements $B' = \{b'_1, \dots, b'_{n_{B'}}\}$. This means that the total number of particles belonging to the B_c graph and they maintain their blue color is $n_{B'}$. Following the same structure, the B_c graph has some particles that became green. Their total number is n_G , they belong to the set G and this set has elements denoted as $G = \{g_1, \dots, g_{n_G}\}$. Considering these facts we have that:

$$\bigotimes_{b \in B_c} \left| \sum_{r \in R} \Gamma_{rb} u_r \right\rangle = \bigotimes_{k \in B_c} |f_k\rangle = \bigotimes_{g \in G} |f_g\rangle \bigotimes_{b \in B'} |f_b\rangle. \quad (21)$$

At this point is useful to recall the definition of the operator $\mathcal{O}_{b, b' \in B_c}$:

$$\mathcal{O}_{b, b' \in B_c} = H^{\dagger \otimes B_c} \left(\prod_{b, b' \in B_c} C_b Z_{b'}^{\Gamma_{bb'}} \right) H^{\otimes B_c} \quad (22)$$

It has to be underlined that the definition of this operator is important to perform the commutation between the daggered Hadamard gates and the corresponding control-Z operations because this is known by the equation (A1). The reason we are defining a separate operator will become obvious at the end of this section. Let us start the

calculation by applying the Hadamard gates:

$$\begin{aligned} & H^{\otimes G} H^{\otimes B'} \bigotimes_{g \in G} |f_g\rangle \bigotimes_{b \in B'} |f_b\rangle \\ &= \sum_{l_{g_1}, \dots, l_{g_{n_G}}=0}^{n_G} \sum_{l_{b_1}, \dots, l_{b_{n_{B'}}}=0}^{n_{B'}} \omega^{\sum_{i=1}^{n_G} l_{g_i} f_{g_i} + \sum_{i=1}^{n_{B'}} l_{b_i} f_{b_i}} \\ & \quad |l_{g_1}, \dots, l_{g_{n_G}}\rangle |l_{b_1}, \dots, l_{b_{n_{B'}}}\rangle \end{aligned}$$

At this point let us mention that for clarity instead of $\sum_{l_{g_1}, \dots, l_{g_{n_G}}=0}^{n_G}$ we are going to write just \sum_{l_g} . Similarly instead $\sum_{l_{b_1}, \dots, l_{b_{n_{B'}}}=0}^{n_{B'}}$ we will write \sum_{l_b} . After these clarifications, we have to proceed with the application of the corresponding control-Z operations. For this, we have to keep in mind the following:

$$\prod_{b, b' \in B_c} CZ^{\Gamma_{bb'}} = \prod_{g \in G, b \in B'} CZ^{\Gamma_{gb}} \quad (23)$$

Therefore we have that:

$$\begin{aligned} & \left(\prod_{g \in G, b \in B'} CZ^{\Gamma_{gb}} \right) H^{\otimes G} H^{\otimes B'} \bigotimes_{g \in G} |f_g\rangle \bigotimes_{b \in B'} |f_b\rangle \\ &= \sum_{l_g} \sum_{l_b} \omega^{\sum_{i=1}^{n_G} l_{g_i} f_{g_i} + \sum_{i=1}^{n_{B'}} l_{b_i} f_{b_i}} \times \omega^{\sum_{i=1}^{n_G} \sum_{j=1}^{n_{B'}} l_{g_i} l_{b_j} \Gamma_{g_i b_j}} \\ & \quad |l_{g_1}, \dots, l_{g_{n_G}}\rangle |l_{b_1}, \dots, l_{b_{n_{B'}}}\rangle \end{aligned}$$

At this point, we assume without loss of generality that $n_G \leq n_{B'}$. Then instead of applying $H^{\dagger \otimes B'} H^{\dagger \otimes G}$, we apply only the $H^{\dagger \otimes B'}$:

$$\begin{aligned} & \left(\prod_{g \in G, b \in B'} CZ^{\Gamma_{gb}} \right) H^{\otimes G} H^{\otimes B'} \bigotimes_{g \in G} |f_g\rangle \bigotimes_{b \in B'} |f_b\rangle \\ &= \sum_{l_g} \sum_{l_b} \sum_{m_b} \omega^{\sum_{i=1}^{n_G} l_{g_i} f_{g_i} + \sum_{i=1}^{n_{B'}} l_{b_i} f_{b_i}} \\ & \quad \times \omega^{\sum_{i=1}^{n_G} \sum_{j=1}^{n_{B'}} l_{g_i} l_{b_j} \Gamma_{g_i b_j}} \omega^{\sum_{i=1}^{n_{B'}} l_{b_i} m_{b_i}} \\ & \quad \times |l_{g_1}, \dots, l_{g_{n_G}}\rangle |m_{b_1}, \dots, m_{b_{n_{B'}}}\rangle \end{aligned}$$

Our goal is to use the property of the Kronecker delta that is given in B using as summation the sums of the l_g indices since they are not a part of the ket in the above equation. To grasp how this works we can have a look at the first element of the summation the l_{b_1} . The relevant terms we are interested in are:

$$l_{b_1} (f_{b_1} + \sum_{i=1}^{n_G} l_{g_i} \Gamma_{b_1 g_i} - m_{b_1}). \quad (24)$$

If we define a quantity p_a as:

$$p_a = f_{b_a} + \sum_{i=1}^{n_G} l_{g_i} \Gamma_{b_a g_i} \quad (25)$$

and take into account the equation (25) we arrive at:

$$\begin{aligned} & H^{\dagger \otimes B'} \left(\prod_{g \in G, b \in B'} CZ^{\Gamma_{gb}} \right) H^{\otimes G} H^{\otimes B'} \bigotimes_{g \in G} |f_g\rangle \bigotimes_{b \in B'} |f_b\rangle \\ &= \sum_{l_g} \sum_{m_b} \delta_{p_1, m_1} \dots \delta_{p_{n_{B'}}, m_{n_{B'}}} \omega^{\sum_{i=1}^{n_G} l_{g_i} f_{g_i}} \\ & \quad |l_{g_1}, \dots, l_{g_{n_G}}\rangle |m_{g_1}, \dots, m_{g_{n_G}}\rangle \end{aligned}$$

and therefore we have that:

$$\begin{aligned} & H^{\dagger \otimes B'} \left(\prod_{g \in G, b \in B'} CZ^{\Gamma_{gb}} \right) H^{\otimes G} H^{\otimes B'} \bigotimes_{g \in G} |f_g\rangle \bigotimes_{b \in B'} |f_b\rangle \\ &= \sum_{l_g} \omega^{\sum_{i=1}^{n_G} l_{g_i} f_{g_i}} |l_{g_1}, \dots, l_{g_{n_G}}\rangle |p_{g_1}, \dots, p_{g_{n_G}}\rangle. \quad (26) \end{aligned}$$

A careful inspection of the equation (26) leads us to write it as:

$$\begin{aligned} & H^{\dagger \otimes B'} \left(\prod_{g \in G, b \in B'} CZ^{\Gamma_{gb}} \right) H^{\otimes G} H^{\otimes B'} \bigotimes_{g \in G} |f_g\rangle \bigotimes_{b \in B'} |f_b\rangle \\ &= \left(\bigotimes_{i=1}^{n_G} Z_{g_i}^{f_{g_i}} \right) \left(\bigotimes_{j=1}^{n_{B'}} X_{b_i}^{f_{b_i}} \right) \\ & \quad \sum_{l_g} |l_{g_1}, \dots, l_{g_{n_G}}\rangle \bigotimes_{m=1}^{n_{B'}} \left| \sum_{k=1}^{n_G} l_{g_k} \Gamma_{b_m g_k} \right\rangle. \quad (27) \end{aligned}$$

At this point, we have to recall the proof of the closed form. Initial for a cleaner presentation of the results let us introduce the Δ operator:

$$\Delta = \left(\bigotimes_{i=1}^{n_G} Z_{g_i}^{f_{g_i}} \right) \left(\bigotimes_{j=1}^{n_{B'}} X_{b_i}^{f_{b_i}} \right). \quad (28)$$

We continue by defining a vector $\vec{g} = (g_1, \dots, g_{n_G})$ and a matrix $\mathcal{G}_{B'} = [\mathbb{I}_{n_R} \mid A_{GB'}^T]$, where $A_{GB'}$ is the part of the general adjacency matrix of the general 3 colorable state we assumed that is of the form $\Gamma_{b,g}$, $b \in B'$ and $g \in G$. At this point become clear the reason the $\mathcal{O}_{b,b' \in B_c}$ operator was defined. Since our main goal is to minimize the number of the terms it becomes apparent that when this operator is applied we need to perform the dagger Hadamards on the color that has more particles in the B_c graph. So after every step, we proved that:

$$\begin{aligned} & H^{\dagger \otimes B_c} H^{\dagger \otimes B_u} |\psi_{3\text{-color}}\rangle = \\ & \quad \sum_{u_1, \dots, u_{n_R}=0}^{d-1} |\vec{u} \mathcal{G}_u^T\rangle \Delta \left(\sum_{g_1, \dots, g_{n_G}=0}^{d-1} |\vec{u} \mathcal{G}_{B'}^T\rangle \right) \quad (29) \end{aligned}$$

which concludes our proof.

B. Discussion of the closed-form expression for the 3-colorable graph.

At this point let us discuss the implications of equation (29). The first is that in reality we have to perform the following operations:

$$H^{\dagger \otimes B'} H^{\dagger \otimes B_u} |\psi_{\text{3-color}}\rangle = \sum_{u_1, \dots, u_{n_R}=0}^{d-1} |\vec{u} \mathcal{G}_u^T\rangle \Delta \left(\sum_{g_1, \dots, g_{n_G}=0}^{d-1} |\vec{u} \mathcal{G}_{B'}^T\rangle \right). \quad (30)$$

This means that our suspicions about whether the result obtained for both 2 and 3 colorable is the corresponding minimal support become stronger, but still this is an endeavor left for future research. Additionally, the form obtained allows us to ask whether it is possible to study the LC/LU/SLOCC equivalency between a 2-colorable graph and a 3-colorable graph generated following our methodology. We have dedicated a section regarding this topic later in this work. Another vital comment is that the number of terms needed to describe the assumed 3-colorable graphs is now $d^{n_R} \times d^{n_G}$. Furthermore, our proof indicates that the theorized 3-colorable graph is written as a quantum orthogonal array (QOA). A QOA is an arrangement having N columns, possibly entangled, such that every reduction to k columns defines a Positive Operator Valued Measure (POVM). Let us recall that POVM is a set of positive semidefinite operators such that they sum up to identity, determining a generalized quantum measurement. Last but not least the form of the equation (30) indicated that the B_c part of the complete 3-colorable graph is the graph basis of the graph. To make our arguments crystal clear let us introduce the adjacency matrix for a general 3-colorable graph:

$$\Gamma_{\text{3-color}} = \begin{pmatrix} \overset{\text{B}}{0} & \overset{\text{R}}{A_{BR}} & \overset{\text{G}}{A_{GR}} \\ \hline \overset{\text{A}_B^T}{A_{BR}} & 0 & \overset{\text{A}_G^T}{A_{GB}} \\ \hline \overset{\text{A}_G^T}{A_{GR}} & \overset{\text{A}_B^T}{A_{GB}} & 0 \end{pmatrix} \quad (31)$$

Here when it is written A_{MN} it means that we have the dedicated block of the adjacency matrix that has every connection between the color N and the color M and has dimensions $n_N \times n_M$. It is possible to write the adjacency matrix for the 3-colorable matrix we have assumed:

$$\Gamma_{\text{3-color}} = \begin{pmatrix} \overset{\text{R}}{0} & \overset{\text{B}_u}{\mathbf{A}_{\mathbf{B}_u \mathbf{R}}} & \overset{\text{B}'}{\mathbf{A}_{\mathbf{B}' \mathbf{R}}} & \overset{\text{G}}{A_{GR}} \\ \hline \overset{\mathbf{A}_{\mathbf{B}_u \mathbf{R}}^T}{0} & 0 & 0 & 0 \\ \hline \overset{\mathbf{A}_{\mathbf{B}' \mathbf{R}}^T}{0} & 0 & 0 & \mathbf{A}_{\mathbf{G} \mathbf{B}'} \\ \hline \overset{\mathbf{A}_{\mathbf{G} \mathbf{R}}^T}{0} & 0 & \mathbf{A}_{\mathbf{G} \mathbf{B}'}^T & 0 \end{pmatrix} \quad (32)$$

Here we have denoted with bold the part of the matrix that makes apparent the condition we have imposed, firstly one has to assume a 2-colorable graph, this is the

top block with bold letters. Then if additional connections are assumed we have the contribution of the additional connections on the 2-colorable graph to make a 3-colorable. Finally, the parts that are non-zero but still not indicated in bold represent the connection of the green and the red particles with the red ones. If this connection is not maintained then we would have ended up with two disconnected diagrams, which axiomatically is not the case for us. A last remark that must be mentioned is that the proof we performed is assuming that we have only one B_c , the presented methodology is still valid if a number of B_c graphs are assumed. For this, we are providing examples in the upcoming sections.

C. Notable 3 colorable families

The goal of this subsection is to study B_c graphs with specific structures that can lead to interesting cases of three-colorable graphs. Let us start by assuming that the B_c graph has the structure given in Figure (6). In this case the $\mathcal{O}_{b,b' \in B_c}$ operator reads:

FIG. 6. 3-colorable straight-line graph with nine vertices.

$$\mathcal{O}_{b,b' \in B_c} = \left(\prod_{k=1}^k H_{b_j}^\dagger \right) \left(\prod_{k=1}^{k-1} C_{b_j} Z_{b_{j+1}}^{\Gamma_{b_j b_{j+1}}} \right) \left(\prod_{k=1}^k H_{b_j} \right). \quad (33)$$

Let us determine the action of the above operator on an arbitrary state $|i_1, \dots, i_k\rangle$:

$$\begin{aligned} & \left(\prod_{k=1}^{k-1} C_{b_j} Z_{b_{j+1}}^{\Gamma_{b_j b_{j+1}}} \right) \left(\prod_{k=1}^k H_{b_j} \right) |i_1, \dots, i_k\rangle \\ &= \sum_{l_1, \dots, l_k=0}^{d-1} \omega^{\sum_{j=1}^k l_j i_j} \times \omega^{\sum_{j=1}^{k-1} l_j l_{j+1} \Gamma_{b_j b_{j+1}}} |l_1, \dots, l_k\rangle \end{aligned}$$

At this point, without loss of generality, it is assumed that the chain contains an odd number of terms. Therefore the last particle is denoted as b_{2k+1} . Bearing in mind the discussion about the number of H^\dagger we can apply to decrease the number of terms only the odd-numbered will be performed and therefore the following is obtained.

$$\begin{aligned} & \left(\prod_{j=0}^k H_{b_{2j+1}}^\dagger \right) \left(\prod_{j=1}^{k-1} C_{b_j} Z_{b_{j+1}}^{\Gamma_{b_j b_{j+1}}} \right) \left(\prod_{j=1}^k H_{b_j} \right) |i_1, \dots, i_k\rangle \\ &= \sum_{l_1, \dots, l_k=0}^{d-1} \sum_{m_1, \dots, m_{2k+1}=0}^{d-1} \omega^{\sum_{j=1}^k l_j i_j - \sum_{j=1}^k m_{2j-1} l_{2j-1}} \\ & \quad \times \omega^{\sum_{j=1}^{k-1} l_j l_{j+1} \Gamma_{b_j b_{j+1}}} |m_1, l_2, m_3, \dots, m_{2k+1}\rangle \end{aligned}$$

Taking into account equation (A3) we arrive at:

$$\mathcal{O}_{b,b' \in B_c} |i_1, \dots, i_k\rangle = \sum_{l_2, \dots, l_{2k}=0}^{d-1} \Omega |i_1 + l_2 \Gamma_{b_1 b_2}, l_2, i_3 + l_2 \Gamma_{b_3 b_2} + l_4 \Gamma_{b_3 b_4}, \dots\rangle.$$

where $\Omega = \omega^{\sum_{j=1}^{d-1} l_{2j} i_{2j}}$. After some algebraic manipulations, it is possible to write it as follows:

$$\mathcal{O}_{b,b' \in B_c} |i_1, \dots, i_k\rangle = \bigotimes_{j=0}^k X_{b_{2j+1}}^{i_{2j+1}} \bigotimes_{j=0}^k Z_{b_{2j}}^{i_{2j}} \sum_{l_2, \dots, l_{2k}=0}^{d-1} |l_2 \Gamma_{b_1 b_2}, l_2, \dots, l_{2k} \Gamma_{b_{2k} b_{2k+1}}\rangle \quad (34)$$

Equation (34) allows for some interesting conclusions. If two particles are assumed the Bell basis is obtained:

$$\mathcal{O}_{b,b' \in B_c} |i, j\rangle = X_{b_1}^i \otimes Z_{b_2}^j \sum_{l=0}^{d-1} |l, l\rangle. \quad (35)$$

As a concrete example, we have that for $d = 2$:

$$\mathcal{O}_{b,b' \in B_c} |i, j\rangle = |i, 0\rangle + (-1)^j |i+1, 1\rangle. \quad (36)$$

This means that the following mapping is obtained, which is the mapping of each one of the combinations to the :

$$\begin{aligned} |00\rangle &\rightarrow |00\rangle + |11\rangle = |\Phi^+\rangle \\ |01\rangle &\rightarrow |00\rangle - |11\rangle = |\Phi^-\rangle \\ |10\rangle &\rightarrow |10\rangle + |01\rangle = |\Psi^+\rangle \\ |11\rangle &\rightarrow -|10\rangle + |01\rangle = -|\Psi^-\rangle \end{aligned} \quad (37)$$

Similarly, for three particles in the chain, the GHZ state is obtained:

$$\mathcal{O}_{b,b' \in B_c} |i_1, i_2, i_3\rangle = X_{b_1}^{i_1} \otimes Z_{b_2}^{i_2} \otimes X_{b_3}^{i_3} \sum_{l=0}^{d-1} |l, l, l\rangle \quad (38)$$

It must be noted that for simplicity in the above example, the values of the adjacency matrix elements are assumed to be one. This is the case as well for the upcoming example where the result for 4 particles is presented

$$\begin{aligned} \mathcal{O}_{b,b' \in B_c} |i_1, i_2, i_3, i_4\rangle &= X_{b_1}^{i_1} \otimes Z_{b_2}^{i_2} \otimes X_{b_3}^{i_3} \otimes Z_{b_4}^{i_4} \\ &\times \sum_{l_2, l_4=0}^{d-1} |l_2, l_2, l_2 + l_4, l_4\rangle. \end{aligned} \quad (39)$$

Using equation (A2) we obtain:

$$\begin{aligned} H_{b_3} H_{b_4}^\dagger \mathcal{O}_{b,b' \in B_c} |i_1, i_2, i_3, i_4\rangle &= \\ X_{b_1}^{i_1} \otimes Z_{b_2}^{i_2} \otimes Z_{b_3}^{i_3} \otimes X_{b_4}^{i_4} &\sum_{l,m=0}^{d-1} \omega^{lm} |l, l\rangle \otimes |m, m\rangle. \end{aligned}$$

This result can be generalized for any number of particles and implies two facts. The first is that indeed the number of H^\dagger operations one should apply for the final step of the calculation of the $\mathcal{O}_{b,b' \in B_c}$ remains $H^{\dagger \otimes B'}$, using our notation and therefore the minimum number of terms for the closed form we found remains the one it was claimed for the general case. The second fact is that it is possible to write part, if not the whole ket inside the 34 as a tensor product of $|l, l\rangle$ or even $|l, l, l\rangle$. This is rather important for the analysis of the LU or the SLOCC equivalence between the state $|\psi_{2\text{-color}}\rangle$ and the state $|\psi_{3\text{-color}}\rangle$.

At this point, it has to be denoted that in the given examples the value of the adjacency matrix is assumed to be one. We recall that every possible value inside the kets belongs to \mathbb{F}_d which is also true for every possible value of the adjacency matrix. It is a well-known mathematical result that the multiplication of any element of a \mathbb{F}_d with any other element maps to an element in \mathbb{F}_d . To grasp this idea one can consider the most simple qudit case, the qutrit ($d=3$). For this assume that every value is $\Gamma = 2$. The possible values inside the brackets are 0, 1, or 2. By multiplying every element with 2 we get, by keeping the order, 0, 2, and 1, and since the order does not matter we have every number only once. This allows us to understand that showing that Bell or GHZ state is obtained assuming every adjacency matrix to be 1 can be generalized for any combination of values for the adjacency matrices.

Let us proceed with the B_C particles creating a circle with an even number of particles to create a two-colorable graph. Equipped with the previously presented results it is easy to conclude that if the B_c graph is an even-numbered circle then the action of the operator $\mathcal{O}_{b,b' \in B_c}$ is given by the following equation:

$$\mathcal{O}_{b,b' \in B_c} |c_1, \dots, c_{2N}\rangle = \bigotimes_{j=0}^k X_{b_{2j+1}}^{c_{2j+1}} \bigotimes_{j=0}^k Z_{b_{2j}}^{c_{2j}} \sum_{l_2, \dots, l_{2N}=0}^{d-1} |l_2 \Gamma_{b_1 b_2} + l_{2N} \Gamma_{b_1 b_{2N}}, l_2, \dots\rangle$$

This result is clearly connected with the obtained in the equation (34), which is expected since the only difference between the first and the second setup is that the first and the last particles are connected in the latter case.

D. Examples of the usage of the obtained closed-form for the 3-colorable graph state

In this subsection, some fruitful examples that make the usage of the obtained formulas clear will be presented. Let us start by assuming a circle with 6 particles. This is done by constructing a 2-colorable graph. At this point we assume that we are connecting two blue particles, see figure 7. This means that the equation to describe the state is:

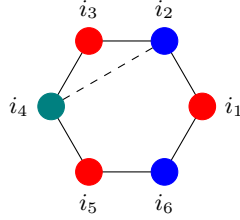


FIG. 7. In this figure we assume a circle with 6 particles, initially a 2-colorable graph. Then two blue vertices are connected (those with indices i_2 and i_4) to create a 3-colorable graph.

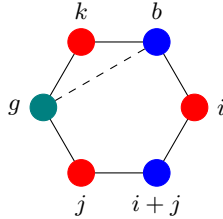


FIG. 8. In this figure we assume a circle with 6 particles, therefore initially a 2 colorable graph. Then two blue vertices are connected (those with indices i_2 and i_4) to create a 3-colorable graph.

$$|\Psi_{GS}\rangle = \sum_{i_1, \dots, i_6=0}^{d-1} \omega^{i_1 i_2} \omega^{i_2 i_3} \omega^{i_3 i_4} \omega^{i_4 i_5} \omega^{i_5 i_6} \omega^{i_6 i_1} \omega^{i_2 i_4} |i_1, i_2, i_3, i_4, i_5, i_6\rangle$$

Using our methodology we arrive at the conclusion that the state can be written as follows if the figure is taken into account:

$$|\psi_{\text{closed-form}}\rangle = \left(\sum_{i,j,k=0}^{d-1} |i\rangle |j\rangle |i+j\rangle \right) X_b^{f_b} \otimes Z_g^{f_g} \sum_{\lambda} |\lambda\rangle_b |\lambda\rangle_g \quad (40)$$

Another fruitful example is the study of the three colorable graph create by assuming one dimensional cluster state with 9 particles and we assume some connections between the blue particles as given in figure 7. The graph state is written as:

$$|\psi_{GS}\rangle = \sum_{i_1, \dots, i_9=0}^{d-1} \left(\prod_{k=1}^8 \omega^{i_k i_{k+1}} \right) \omega^{i_1 i_9} \omega^{i_5 i_7} |i_1, \dots, i_9\rangle \quad (41)$$

If the obtained closed form is obtained we can remain the indices like in the figure 10 and the state can be written as following:

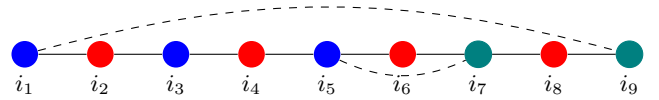


FIG. 9. A sequence of circles connected by edges, alternating in blue and red.

$$|\psi_{\text{closed-form}}\rangle = \left(\sum_{i,j,k,l=0}^{d-1} |i\rangle |i+j\rangle |j\rangle |k\rangle |l\rangle \right) \left(X_{b_1}^{f_{b_1}} \otimes Z_{g_1}^{f_{g_1}} \sum_{\lambda=0}^{d-1} |\lambda\rangle_{b_1} |\lambda\rangle_{g_1} \right) \left(X_{b_2}^{f_{b_2}} \otimes Z_{g_2}^{f_{g_2}} \sum_{\lambda=0}^{d-1} |\lambda\rangle_{b_2} |\lambda\rangle_{g_2} \right)$$

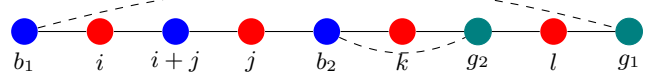


FIG. 10. A sequence of circles connected by edges, alternating in blue and red.

This example does not explain how our formula can be used for the 3-colorable case but also shows how it can be adapted if we have more than one region within the original 2-colorable graph where particles of the same color are connected to make a new three-colorable graph. In this case, the simplest example is studied, where only 2 vertices are connected.

V. LU OR SLOCC EQUIVALENCE

A. Equivalence classes under Local Unitary Operators

Entanglement characterization is crucial when graph states are studied [13]. For this, the examination of the equivalence classes arises naturally. Another physical reason to address this issue is that graph states emerge in network scenarios for which each vertex is theorized to be separated qudit or a lab and the spatial distance between them is large enough not to allow for joint operations [29]. Therefore we have to assume that the quantum operations \mathcal{E} are a subclass of completely positive maps (CPM) that are separable if the finest partitioning is assumed. In our case, we are interested in the transformation from state $|\psi_1\rangle$ to $|\psi_2\rangle$ with a non-zero probability if a CPM \mathcal{E} is adopted. Characterizing the complete class of every transformation \mathcal{E} that belongs to the Local Operations and Classical Communications (LOCC) is broad and generally challenging. Usually, it is assumed that:

$$\mathcal{E}(\rho) = \bigotimes_{j=1}^N \mathcal{E}_j^{(j)} \rho \bigotimes_{j=1}^N \mathcal{E}_j^{(j)\dagger}, \quad (42)$$

which means that: $|\psi_2\rangle = \bigotimes_{j=1}^N \mathcal{E}_j^{(j)} |\psi_1\rangle$. For clarification:

$$\bigotimes_{j=1}^N \mathcal{E}_j^{(j)} = \mathcal{E}_1^{(1)} \otimes \cdots \otimes \mathcal{E}_N^{(N)} \quad (43)$$

At this point let us present three dissimilar classes of local operations[13]. The first one is the invertible Stochastic LOCC (SLOCC), which means that the operation performed in each qudit is of the form $\mathcal{E}_i \in \text{SL}(2, \mathbb{C})$. The probability of achieving an SLOCC transformation is typically less than one. Then the Local Uninatry (LU) equivalence must be taken into account, which means that each operation on every qudit is $\mathcal{E}_i \in U(2)$. Finally, the Local Clifford Unitaries are operations one each qudit such that $\mathcal{E}_i \in \mathcal{C}_1$, which means they are one of the Clifford unitaries[33]. The last two have the probability to be achieved, if exist, equal to unity.

1. Graphical Rule for the LC equivalence

At this point deepening our focus on the LC equivalence is vital to understand vital consequences of our work. The generalized Pauli group is generated as follows [33]:

$$\mathcal{P} = \{\omega^a X^b Z^c\}, \quad \text{with } a, b, c \in \mathbb{F}_d \quad (44)$$

The n-body Pauli group \mathcal{P}_n is defined as the tensor product of \mathcal{P} . Then the Clifford group for n particles \mathcal{C}_n can be presented which is the normalizer of the \mathcal{P}_n . It is noteworthy that for qubits there is a simple graphical rule to determine and examine if two graph states are LC equivalent [40] and is called Local Complementation [41]. The rule is rather simple, one has to choose a vertex a . Then the neighborhood N_a of a must be checked. If the two vertices are connected the edges are deleted if they are not a connection is established. Additionally, it was shown in [32] that the aforementioned rule can be written in terms of local unitaries as follows:

$$\text{LC}_a = \sqrt{-iX_a} \bigotimes_{b \in N_a} \sqrt{iZ_b} \quad (45)$$

It is worth mentioning that the idea of local complementation has been extended to qudits [33] but the corresponding local transformations are not found. It must be noted that if two graph states are not LC equivalent this does not imply that they are also not LC equivalent, if the number of particles is above 8 as it was shown in [42]. In [28] an approach to construct examples for this case is presented. Finally, one has to bear in mind that the application of local Clifford operations on a graph state does not necessarily lead to a graph state directly, but in general, it should be a stabilizer state [29]. But since stabilizer states can be realized as graph states as it was shown in [14] every stabilizer state is LC equivalent to some graph state. A final remark is that even if an

efficient algorithm for graphs has been developed [41] as well as the algorithm for the determination of two stabilizer states are LC equivalent the endeavor of increasing the number of particles and finding the LC orbit for a large number of particles turns out to be a challenging goal [43].

B. Distinct examples and LU or SLOCC equivalence between the 2 and 3 colorable graphs

In this section a vital question will be addressed, are the 2-colorable graph state $|\psi_{2\text{-color}}\rangle$ and an arbitrary, but generated with our rule, 3-colorable graph state $|\psi_{3\text{-color}}\rangle$ SLOCC, LU, or even LC equivalent? Addressing this question for the most general case of $|\psi_{2\text{-color}}\rangle$ and therefore $|\psi_{3\text{-color}}\rangle$ is challenging but it turns out that the bibliography offers a great variety of studied states that belong to the category we theorized. In this section, a collection of cases that are developed in the literature and satisfy the conditions we imposed is presented. Let us start recalling the complete bipartite graph state. For this, figure 11 can be taken into account.

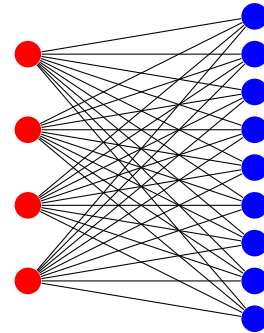


FIG. 11. Complete bipartite graph with $n_R = 4$ red vertices and $n_B = 9$ blue vertices.

It is shown that this state is a k-uni state [35], for more details on k-uni states one could refer to the aforementioned work. The main idea is that in this case the adjacency matrix of $|\psi_{2\text{-color}}\rangle$ is:

$$\Gamma_{2\text{-color}} = \left(\begin{array}{c|c} \overset{\text{B}}{\overset{\text{O}}{\overbrace{\quad}}} & \overset{\text{R}}{\overset{\text{A}}{\overbrace{\quad}}} \\ \hline \overset{\text{A}^T}{\overset{\text{O}}{\overbrace{\quad}}} & \overset{\text{O}}{\overset{\text{O}}{\overbrace{\quad}}} \end{array} \right) \quad (46)$$

with the only restriction being that all submatrices of A must be non-singular. Then if a number of blue particles are taken to form a new bipartite graph as in figure (12), keeping their initial connections the new graph that occurs is not SLOCC equivalent to the previous one.

From the same work is deducted that if the initial number of particles in the initial 2-colorable complete bipartite graph ($|\psi_{2\text{-color}}\rangle$) is odd and only one connection is assumed to create a new 3-colorable graph like in the figure (13) these states are not SLOCC equivalent.

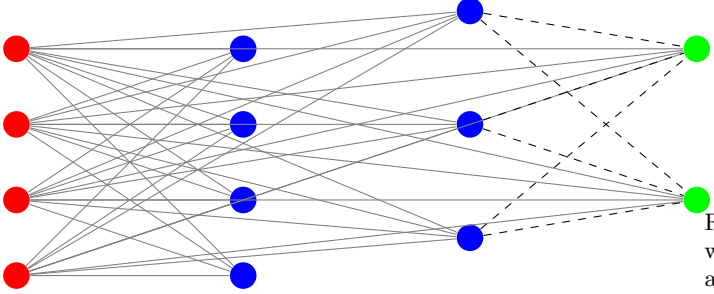


FIG. 12. How an initial complete bipartite graph with 4 red particles and 9 blue particles transformed into a three-colorable one. On the left, we have the red particles. In the middle, the blue particles which did not participate in additional connects are given (B_u set) while on the left the B_c is given where a new bipartite subgraph is created.

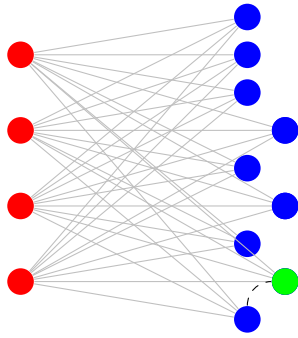


FIG. 13. How an initial complete bipartite graph with 4 red particles and 9 blue particles transformed into a three-colorable one. Two particles belong to the B_c set creating additional terms in the reduced closed form emerging from the 2 colorable cases which belong to the Bell basis.

Let us proceed with another fruitful example found in the literature. In [29] it was shown that the two-colorable graph given in figure (14) is not LU equivalent to the graph given in the figure (15). It is clear that the obtained three-colorable graph is exactly a simple example of the class of three-colorable graphs we are interested in.

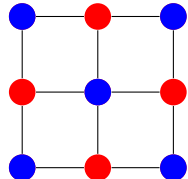


FIG. 14. Cluster state with the particles arranged in a 3×3 grid.

Finally, examples that the 2-colorable and three-colorable graphs are not LU equivalent can be found in figures 4 and 5 by [32]. These examples prove that our condition creates different families of graph states that are particularly interesting in the literature in various instances. This motivates us to provide examples interest-

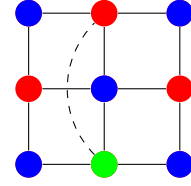


FIG. 15. A three-colorable graph state created by starting with cluster state with the particles arranged in a 3×3 grid and then connecting two particles of the same color.

ing for future study and this is the aim of the upcoming session.

VI. FUTURE OUTLOOK

In this section, the future outlook of this work will be discussed. In each case, the title of the subsection is referred to the type of the basis 2-colorable assumed. As it became clear from the previous section our future aim is to examine the SLOCC/LU/LC equivalency between any 2-colorable graph state $|\psi_{2\text{-color}}\rangle$ and an arbitrary, but generated with our rule, 3-colorable graph state $|\psi_{3\text{-color}}\rangle$.

A. k-UNI states

The k-UNI states are pure quantum states which are highly entangled with the special property that all of their k-qudit reduced density matrices are maximally mixed. The complete bipartite graph is an example of a k-UNI state and is given in figure (11). It is a 2 colorable and the 3 colorable is a graph where the particles in B_c for pairs like in figure (16) should be studied. One has to keep in mind that in this case products of states from a Bell basis are obtained. Then it can be assumed that the particles belonging to the B_c set are forming a chain like is depicted in the figure (17). Finally, the exploration of any possible combination of chains or circles existing for the particles belonging to the B_c set is a rational extension to this work.

B. n-GHZ state

Another interesting case of study is the initial 2-colorable graph is a star-shaped graph like the one given in the figure (18).

The corresponding graph state is LU equivalent to the fully connected graph state [13] and the GHZ state [29]. The n-particle GHZ state is given by the following equation:

$$|\text{GHZ}_n\rangle = \frac{1}{\sqrt{2}}(|00\cdots 0\rangle + |11\cdots 1\rangle). \quad (47)$$

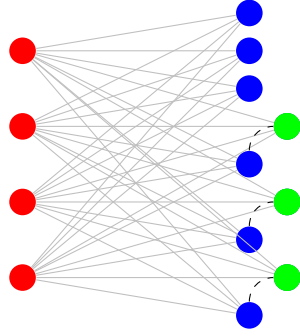


FIG. 16. How an initial complete bipartite graph with 4 red particles and 9 blue particles transformed into a three-colorable one. Six particles belong to the B_c set creating additional terms in the reduced closed form emerging from the 2 colorable cases which belong to the Bell basis.

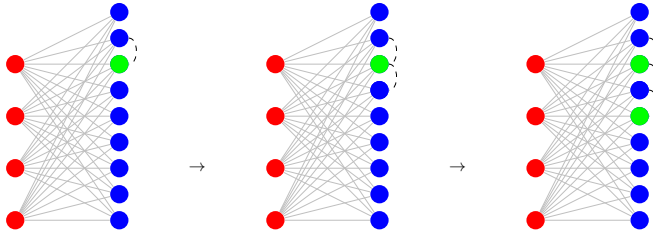


FIG. 17. Progressive creation of a chain for the particles in the B_c set to create one chain.

If we assume that every particle apart from the central one creates a pair with the one next to it (figure (19)) then the corresponding graph is called a friendship graph in graph theory [44] and therefore the examination of the SLOCC/LU/LC between the star shape graph and the corresponding quantum friendship graph arises as a natural question.

C. Cluster states

Another interesting instance one should examine is if the initial 2 colorable graph is a cluster state like the example in figure (20). Then it is meaningful to examine the creation of various chains among the particles belonging to the B_c . In figure (21) we have added only 2-body connections but of course, the number of particles can increase. Additionally, it is possible to have chains of different lengths or even circles, like in Figure (22) to be created among the particles belonging to the B_c set.

D. Open question: LC orbits for qudits

Trying to address a closed form for a general three-colorable graph is not trivial. The reason we focused on the imposed methodology is dual. Initially, the result for the 2-colorable case can be directly implemented in our

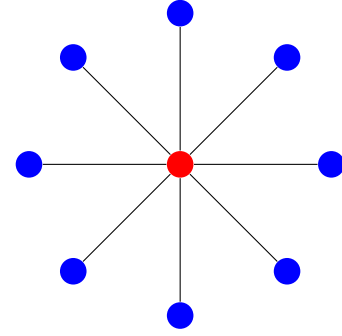


FIG. 18. Star-shaped diagram with $n_B = 1$ red central particle and $n_B = 8$ blue surrounding particles.

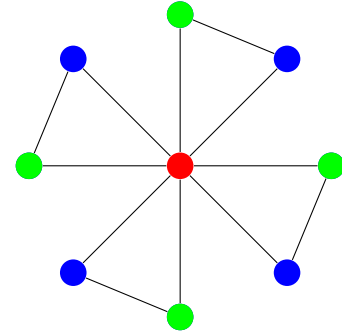
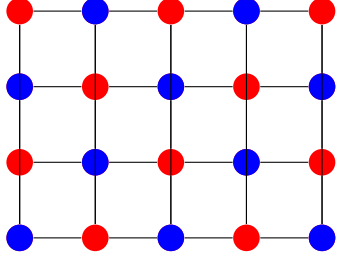
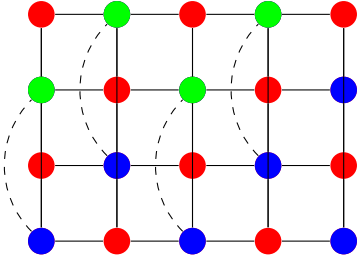


FIG. 19. A graph state with the corresponding graph to be a friendship graph.

three-colorable case making it possible to derive closed form as well. Secondly, it could be helpful to assist in the effort of exploring the LC orbits of graph states with a higher number of particles than the one presented in [43]. As it is stated the computational challenges of this task are great. Apart from the implementation improvements that can assist in the increase of the number of particles used, it is also possible to increase the number of particles but restrict ourselves to examples with an application direction. By this, it is implied that if a network of distant labs is theorized and this is two colorable graphs having a catalog of the SLOCC equivalent configuration will be of great impact to decide where to build or how to connect the aforementioned lab. Finally, it is crucial to ask if a general approach to check if two states are equivalent if they are the same apart from two subgraphs that it is proven are not LU equivalent. The most prominent question to be answered is if the graphical rule to compare two qudit graph states present by [33] is possible to be written as local quantum operators. Then the approaches presented in the previous paragraph could be extended for the d-level systems.

VII. CONCLUSIONS

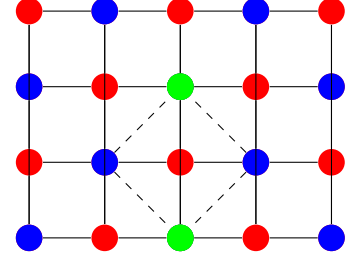
In this work, we have presented closed-form expressions for arbitrary two-colorable graph states in qudit

FIG. 20. A cluster state organized in a 5×4 grid.FIG. 21. A three-colorable graph state created using a cluster state organized in a 5×4 grid as the 2-colorable bases. Here only two body chains are assumed

systems, where the number of terms is d^{n_R} , with n_R representing the number of red particles. This result underscores the significance of colorability in simplifying the representation of graph states and enhancing their practical applications in quantum information processing. Our findings show that the closed-form expression of these states is tightly linked to the graph structure and the distribution of particles in red n_R and blue n_B .

We extended our analysis to a broad family of three-colorable graph states, constructed from two two-colorable graph states. The closed-form expression for these states is in the form of one two-colorable state tensor product with the graph basis formed from another two-colorable state. This approach systematically reduces the number of terms required to represent these states, further highlighting the practical advantages of studying colorability.

Specific examples were provided to illustrate instances where the LU (Local Unitary) or SLOCC (Stochastic Local Operation and Classical Communication) equivalence of two-colorable and corresponding three-colorable states were demonstrated. The future outlook of this work is showcasing interesting cases for which the local operation equivalency should be studied. Understanding these equivalencies is crucial for the technological applications of quantum technologies, particularly in quantum error correction, multi-party quantum communication, and quantum computation.

FIG. 22. A three-colorable graph state created using a cluster state organized in a 5×4 grid as the 2-colorable bases. Here the particles belonging to the B_c set are creating a circle.

ACKNOWLEDGMENTS

We thank Edwin Barnes, Sophia Economou, Mario Flory, Otfried Gühne, Géza Tóth, and Karol Życzkowski for their valuable discussions and remarks.

Appendix A: Some useful Properties

Let us present some useful for our analysis relations. The first one is the commutation of $H^\dagger CZ |kj\rangle$, which is given by the following equation:

$$H^\dagger CZ |kj\rangle = CXH^\dagger |kj\rangle, \quad (A1)$$

and it is proven in the Appendix B. Another useful property that the X operator to the power $a \in \mathbb{F}_d$ is given by the following equation:

$$X^a = H^\dagger Z^a H. \quad (A2)$$

The above property is proven in the Appendix C. Finally a mathematical fact we are going to use extensively in our analysis is:

$$\frac{1}{N} \sum_l \left(\exp \left(\frac{2\pi i}{N} (k-j) \right) \right)^l = \delta_{k,j}, \quad \text{for } k, j \in \mathbb{Z}, \quad (A3)$$

Appendix B

Let us assume a two-body state $|k, j\rangle$ with $k, j \in \mathbb{Z}_d$, where d is the local dimension.

$$H^\dagger CZ |kj\rangle = \omega^{kj} H^\dagger |kj\rangle = \frac{1}{\sqrt{d}} \omega^{kj} |k\rangle \sum_{l=0}^{d-1} \omega^{-lj} |l\rangle \quad (B1)$$

On the other hand, let us apply the following:

$$\begin{aligned}
CXH^\dagger |kj\rangle &= \frac{1}{\sqrt{d}} CX |k\rangle \sum_{l=0}^{d-1} \omega^{-lj} |l\rangle \\
&= \frac{1}{\sqrt{d}} |k\rangle \sum_{l=0}^{d-1} \omega^{-lj} |l+k\rangle \\
&= \frac{1}{\sqrt{d}} |k\rangle \sum_{l=0}^{d-1} \omega^{kj} \omega^{-kj} \omega^{-lj} |l+k\rangle \\
&= \frac{1}{\sqrt{d}} \omega^{kj} |k\rangle \sum_{l=0}^{d-1} \omega^{-(l+k)j} |l+k\rangle \\
&= \frac{1}{\sqrt{d}} \omega^{kj} |k\rangle \sum_{l'=0}^{d-1} \omega^{-l'j} |l'\rangle. \quad (\text{B2})
\end{aligned}$$

Therefore the proof is completed.

Appendix C

The application of X^a yields $X^a |i\rangle = |i+a\rangle$. While for the $H^\dagger Z^a H$ we have:

$$\begin{aligned}
H |i\rangle &= \sum_{l=0}^{d-1} \omega^{il} |l\rangle \\
Z^a H |i\rangle &= \sum_{l=0}^{d-1} \omega^{il} \omega^{al} |l\rangle \\
H^\dagger Z^a H |i\rangle &= \sum_{m=0}^{d-1} \sum_{l=0}^{d-1} \omega^{il} \omega^{al} \omega^{-ml} |m\rangle,
\end{aligned}$$

which leads to $H^\dagger Z^a H |i\rangle = |i+a\rangle$ and therefore the proof is completed.

[1] Ryszard Horodecki, Paweł Horodecki, Michał Horodecki, and Karol Horodecki. Quantum entanglement. *Reviews of Modern Physics*, 81(2):865–942, June 2009. ISSN 1539-0756. doi:10.1103/revmodphys.81.865. URL <http://dx.doi.org/10.1103/RevModPhys.81.865>.

[2] W. Dür, G. Vidal, and J. I. Cirac. Three qubits can be entangled in two inequivalent ways. *Physical Review A*, 62(6), November 2000. ISSN 1094-1622. doi:10.1103/physreva.62.062314. URL <http://dx.doi.org/10.1103/PhysRevA.62.062314>.

[3] F. Verstraete, J. Dehaene, B. De Moor, and H. Verschelde. Four qubits can be entangled in nine different ways. *Physical Review A*, 65(5), April 2002. ISSN 1094-1622. doi:10.1103/physreva.65.052112. URL <http://dx.doi.org/10.1103/PhysRevA.65.052112>.

[4] Emmanuel Briand, Jean-Gabriel Luque, Jean-Yves Thibon, and Frank Verstraete. The moduli space of three-qutrit states. *Journal of Mathematical Physics*, 45(12):4855–4867, December 2004. ISSN 1089-7658. doi:10.1063/1.1809255. URL <http://dx.doi.org/10.1063/1.1809255>.

[5] Martin Hebenstreit, Cornelia Spee, Nicky Kai Hong Li, Barbara Kraus, and Julio I. de Vicente. State transformations within entanglement classes containing permutation-symmetric states. *Physical Review A*, 105(3), March 2022. ISSN 2469-9934. doi:10.1103/physreva.105.032458. URL <http://dx.doi.org/10.1103/PhysRevA.105.032458>.

[6] A. J. Scott. Multipartite entanglement, quantum-error-correcting codes, and entangling power of quantum evolutions. *Phys. Rev. A*, 69:052330, May 2004. doi:10.1103/PhysRevA.69.052330. URL <https://link.aps.org/doi/10.1103/PhysRevA.69.052330>.

[7] Zahra Raissi, Christian Gogolin, Arnaud Riera, and Antonio Acín. Optimal quantum error correcting codes from absolutely maximally entangled states. *Journal of Physics A: Mathematical and Theoretical*, 51(7):075301, January 2018. ISSN 1751-8121. doi:10.1088/1751-8121/aaa151. URL <http://dx.doi.org/10.1088/1751-8121/aaa151>.

[8] Zahra Raissi, Adam Teixidó, Christian Gogolin, and Antonio Acín. Constructions of k -uniform and absolutely maximally entangled states beyond maximum distance codes. *Physical Review Research*, 2(3), September 2020. ISSN 2643-1564. doi:10.1103/physrevresearch.2.033411. URL <http://dx.doi.org/10.1103/PhysRevResearch.2.033411>.

[9] Adam Burchardt and Zahra Raissi. Stochastic local operations with classical communication of absolutely maximally entangled states. *Physical Review A*, 102(2), August 2020. ISSN 2469-9934. doi:10.1103/physreva.102.022413. URL <http://dx.doi.org/10.1103/PhysRevA.102.022413>.

[10] Zahra Raissi, Adam Burchardt, and Edwin Barnes. General stabilizer approach for constructing highly entangled graph states. *Physical Review A*, 106(6), December 2022. ISSN 2469-9934. doi:10.1103/physreva.106.062424. URL <http://dx.doi.org/10.1103/PhysRevA.106.062424>.

[11] Zahra Raissi, Edwin Barnes, and Sophia E. Economou. Deterministic generation of qudit photonic graph states from quantum emitters. *PRX Quantum*, 5:020346, May 2024. doi:10.1103/PRXQuantum.5.020346. URL <https://link.aps.org/doi/10.1103/PRXQuantum.5.020346>.

[12] Hrachya Zakaryan, Konstantinos-Rafail Revis, and Zahra Raissi. Non-symmetric ghz states; weighted hypergraph and controlled-unitary graph representations, 2024. URL <https://arxiv.org/abs/2408.02740>.

[13] M. Hein, W. Dür, J. Eisert, R. Raussendorf, M. Van den Nest, and H. J. Briegel. Entanglement in graph states and its applications, 2006.

[14] D. Schlingemann. Stabilizer codes can be realized as graph codes, 2001. URL <https://arxiv.org/abs/quant-ph/0111080>.

[15] Robert Raussendorf, Daniel Browne, and Hans Briegel. The one-way quantum computer—a non-network model of quantum computation. *Journal of*

Modern Optics, 49(8):1299–1306, July 2002. ISSN 1362-3044. doi:10.1080/09500340110107487. URL <http://dx.doi.org/10.1080/09500340110107487>.

[16] Sara Bartolucci, Patrick Birchall, Hector Bombin, Hugo Cable, Chris Dawson, Mercedes Gimeno-Segovia, Eric Johnston, Konrad Kieling, Naomi Nickerson, Mihir Pant, Fernando Pastawski, Terry Rudolph, and Chris Sparrow. Fusion-based quantum computation, 2021. URL <https://arxiv.org/abs/2101.09310>.

[17] M. Zwerger, H. J. Briegel, and W. Dür. Measurement-based quantum communication. *Applied Physics B*, 122(3), March 2016. ISSN 1432-0649. doi:10.1007/s00340-015-6285-8. URL <http://dx.doi.org/10.1007/s00340-015-6285-8>.

[18] Daniel Gottesman. An introduction to quantum error correction and fault-tolerant quantum computation, 2009. URL <https://arxiv.org/abs/0904.2557>.

[19] W. Dür, H. Aschauer, and H.-J. Briegel. Multiparticle entanglement purification for graph states. *Phys. Rev. Lett.*, 91:107903, Sep 2003. doi:10.1103/PhysRevLett.91.107903. URL <https://link.aps.org/doi/10.1103/PhysRevLett.91.107903>.

[20] Gérard D. Cohen, Iiro S. Honkala, Simon Litsyn, and Antoine Lobstein. Covering codes. In *North-Holland Mathematical Library*, 2005. URL <https://api.semanticscholar.org/CorpusID:195891379>.

[21] Simone Severini. Two-colorable graph states with maximal schmidt measure. *Physics Letters A*, 356(2):99–103, July 2006. ISSN 0375-9601. doi:10.1016/j.physleta.2006.03.026. URL <http://dx.doi.org/10.1016/j.physleta.2006.03.026>.

[22] David Sauerwein, Katharina Schwaiger, and Barbara Kraus. Discrete and differentiable entanglement transformations, 2018. URL <https://arxiv.org/abs/1808.02819>.

[23] B. Kraus. Local unitary equivalence of multipartite pure states. *Phys. Rev. Lett.*, 104:020504, Jan 2010. doi:10.1103/PhysRevLett.104.020504. URL <https://link.aps.org/doi/10.1103/PhysRevLett.104.020504>.

[24] Matthew J. Donald, Michał Horodecki, and Oliver Rudolph. The uniqueness theorem for entanglement measures. *Journal of Mathematical Physics*, 43(9):4252–4272, 09 2002. ISSN 0022-2488. doi:10.1063/1.1495917. URL <https://doi.org/10.1063/1.1495917>.

[25] David Gunn, Martin Hebenstreit, Cornelia Spee, Julio I. de Vicente, and Barbara Kraus. Approximate and ensemble local entanglement transformations for multipartite states. *Physical Review A*, 108(5), November 2023. ISSN 2469-9934. doi:10.1103/physreva.108.052401. URL <http://dx.doi.org/10.1103/PhysRevA.108.052401>.

[26] David Sauerwein, Nolan R. Wallach, Gilad Gour, and Barbara Kraus. Transformations among pure multipartite entangled states via local operations are almost never possible. *Phys. Rev. X*, 8:031020, Jul 2018. doi:10.1103/PhysRevX.8.031020. URL <https://link.aps.org/doi/10.1103/PhysRevX.8.031020>.

[27] Antoine Neven, David Gunn, Martin Hebenstreit, and Barbara Kraus. Local transformations of multiple multipartite states. *SciPost Phys.*, 11:042, 2021. doi:10.21468/SciPostPhys.11.2.042. URL <https://scipost.org/10.21468/SciPostPhys.11.2.042>.

[28] Nikoloz Tsimakuridze and Otfried Gühne. Graph states and local unitary transformations beyond local clifford operations. *Journal of Physics A: Mathematical and Theoretical*, 50(19):195302, April 2017. ISSN 1751-8121. doi:10.1088/1751-8121/aa67cd. URL <http://dx.doi.org/10.1088/1751-8121/aa67cd>.

[29] Lina Vandré, Jarn de Jong, Frederik Hahn, Adam Burchardt, Otfried Gühne, and Anna Pappa. Distinguishing graph states by the properties of their marginals, 2024. URL <https://arxiv.org/abs/2406.09956>.

[30] Douglas B. West. Prentice Hall, Upper Saddle River, N.J., second edition, 2001. ISBN 0130144002 9780130144003.

[31] Reinhard Diestel. *Graph Theory (Graduate Texts in Mathematics)*. Springer, 2005. ISBN 3540261826.

[32] M. Hein, J. Eisert, and H. J. Briegel. Multipartite entanglement in graph states. *Physical Review A*, 69(6), June 2004. ISSN 1094-1622. doi:10.1103/physreva.69.062311. URL <http://dx.doi.org/10.1103/PhysRevA.69.062311>.

[33] Mohsen Bahramgiri and Salman Beigi. Graph states under the action of local clifford group in non-binary case, 2007. URL <https://arxiv.org/abs/quant-ph/0610267>.

[34] F. J. (Florence Jessie) MacWilliams and N. J. A. (Neil James Alexander) Sloane. *The Theory of Error Correcting Codes*. North-Holland Pub. Co.; sole distributors for the U.S.A. and Canada, Elsevier/North-Holland, 1977. ISBN 0444850090.

[35] Zahra Raissi, Adam Burchardt, and Edwin Barnes. General stabilizer approach for constructing highly entangled graph states. *Physical Review A*, 106(6), December 2022. ISSN 2469-9934. doi:10.1103/physreva.106.062424. URL <http://dx.doi.org/10.1103/PhysRevA.106.062424>.

[36] Dardo Goyeneche, Zahra Raissi, Sara Di Martino, and Karol Życzkowski. Entanglement and quantum combinatorial designs. *Phys. Rev. A*, 97:062326, Jun 2018. doi:10.1103/PhysRevA.97.062326. URL <https://link.aps.org/doi/10.1103/PhysRevA.97.062326>.

[37] Richard M. Karp. *Reducibility among Combinatorial Problems*, pages 85–103. Springer US, Boston, MA, 1972. ISBN 978-1-4684-2001-2. doi:10.1007/978-1-4684-2001-2_9. URL https://doi.org/10.1007/978-1-4684-2001-2_9.

[38] L. Stockmeyer. Planar 3-colorability is polynomial complete. *SIGACT News*, 5(1), 1973.

[39] L. Lovasz. Coverings and colorings of hypergraphs. In *Proceedings of the 4th Southeastern Conference on Combinatorics, Graph Theory, and Computing*, pages 3–12, 1973. URL <http://www.cs.elte.hu/~lovasz/scans/covercolor.pdf>.

[40] Maarten Van den Nest, Jeroen Dehaene, and Bart De Moor. Graphical description of the action of local clifford transformations on graph states. *Physical Review A*, 69(2), February 2004. ISSN 1094-1622. doi:10.1103/physreva.69.022316. URL <http://dx.doi.org/10.1103/PhysRevA.69.022316>.

[41] André Bouchet. Recognizing locally equivalent graphs. *Discrete Mathematics*, 114(1):75–86, 1993. ISSN 0012-365X. doi:10.1016/0012-365X(93)90357-Y. URL [https://doi.org/10.1016/0012-365X\(93\)90357-Y](https://doi.org/10.1016/0012-365X(93)90357-Y).

[42] Zhengfeng Ji, Jianxin Chen, Zhaohui Wei, and Ming-sheng Ying. The lu-lc conjecture is false, 2008. URL <https://arxiv.org/abs/0709.1266>.

- [43] Jeremy C. Adcock, Sam Morley-Short, Axel Dahlberg, and Joshua W. Silverstone. Mapping graph state orbits under local complementation. *Quantum*, 4:305, August 2020. ISSN 2521-327X. doi:10.22331/q-2020-08-07-305. URL <http://dx.doi.org/10.22331/q-2020-08-07-305>.
- [44] Paul L. Erdos and Joel H. Spencer. Paul erdös : the art of counting : selected writings. 1973. URL <https://api.semanticscholar.org/CorpusID:60087231>.